TEM-1 β-Lactamase Folds in a Nonhierarchical Manner with Transient Non-Native Interactions Involving the C-Terminal Region†

Annabelle Lejeune,‡,§ Roger H. Pain,|| Paulette Charlier,‡ Jean-Marie Frère,‡ and André Matagne*,‡

Laboratoire d'Enzymologie and Laboratoire de Cristallographie des Protéines, Centre for Protein Engineering, Université de Liège, Institut de Chimie B6, 4000 Liège (Sart Tilman), Belgium, and Department of Biotechnology, Jožef Stefan Institute, Ljubljana, Slovenia

Received September 21, 2007; Revised Manuscript Received November 27, 2007

ABSTRACT: The conformational stability and kinetics of refolding and unfolding of the W290F mutant of TEM-1 β-lactamase have been determined as a function of guanidinium chloride concentration. The activity and spectroscopic properties of the mutant enzyme did not differ significantly from those of the wild type, indicating that the mutation has only a very limited effect on the structure of the protein. The stability of the folded protein is reduced, however, by 5−10 kJ mol^{-1} relative to that of the molten globule intermediate (H), but the values of the folding rate constants are unchanged, suggesting that Trp-290 becomes organized in its nativelike environment only after the rate-limiting step; i.e., the C-terminal region of the enzyme folds very late. In contrast to the significant increase in fluorescence intensity seen in the dead time (3−4 ms) of refolding of the wild-type protein, no corresponding burst phase was observed with the mutant enzyme, enabling the burst phase to be attributed specifically to the C-terminal Trp-290. This residue is suggested to be buried in a nonpolar environment from which it has to escape during subsequent folding steps. With both proteins, fast early collapse leads to a folding intermediate in which the C-terminal region of the polypeptide chain is trapped in a non-native structure, consistent with a nonhierarchical folding process.

β-Lactamases very efficiently catalyze the hydrolysis of the β-lactam ring of penicillins and related compounds. Synthesis of one or more of these enzymes constitutes the most common, and often the most effective, mechanism employed by bacteria to escape the action of β-lactam antibiotics (*1*, *2*). Many β-lactamases have been described and divided, on the basis of their primary structures, into four classes, A, B, C, and D (*3*).

TEM-1 class A β-lactamase (Figure 1) is a widespread plasmid-encoded monomeric protein comprising 265 amino acid residues (M_r = 28 907) organized into two structural domains (an all-α domain and an α/β domain), with the active site serine (Ser-70) situated in a cleft between the two domains (*4*−*6*). The all-α domain is formed by the central part of the polypeptide chain (residues 69−212), and the α/β domain is composed of the N- and C-terminal extensions of the α domain, which intertwine to form a five-stranded β-pleated sheet. The enzyme contains 12 prolyl residues (one of which is in a *cis* conformation in the native state) and a single disulfide bond connecting Cys-77 and Cys-123 in the all-α domain. It contains four tryptophan residues at positions 165, 210, 229, and C-terminal 290. The folding properties of TEM-1 have been characterized in some detail (*7*−*10*). As with most proteins with more than 100 amino acids (*11*), folding is not kinetically two-state and intermediate, partially folded species are observed. Formation of the native state of TEM-1, monitored by intrinsic fluorescence and recovery of enzymatic activity, occurs with biphasic kinetics, which indicates that the enzyme folds via two major parallel pathways (*9*), both rate-limited by *cis*−*trans* isomerization of Xaa−Pro peptide bonds. In particular, the slowest refolding phase (τ = 200−300 s at 25 °C) has been associated with the *trans* to *cis* isomerization of the Glu-166−Pro-167 bond in the Ω-loop (*9*) (see Figure 1). The use of a variety of complementary spectroscopic techniques, including intrinsic and extrinsic fluorescence and far-UV[1] circular dichroism (CD) (*10*), has provided evidence of submillisecond hydrophobic collapse, with formation of substantial amounts of secondary structure. This leads to an early intermediate characterized by non-native elements of structure, which have to rearrange in later steps of folding, thus indicating a nonhierarchical folding pathway. An attractive model put forward by Vanhove et al. (*10*) involves inclusion of the C-terminal Trp-290 in a non-native conformation in

† This work was supported in part by grants from the Fonds de la Recherche Fondamentale et Collective (Contracts 2.4550.05, 2.4.524.03, and 2.4511.06) and by the Belgian program of Interuniversity Attraction Poles initiated by the Federal Office for Scientific Technical and Cultural Affairs (PAI n° P5/33 and P6/19). A.L. was the recipient of a FRIA fellowship (09/1995-01/2000). A.M. is Research Associate of the National Fund for Scientific Research (FRS-FNRS, Belgium).

* To whom correspondence should be addressed. E-mail: amatagne@ulg.ac.be. Telephone: +32(0)43663419. Fax: +32(0) 43663364.

‡ Université de Liège.

§ Present address: Dyax s.a., Institut de Botanique, Building 22, Bd du Rectorat 27B, 4000 Liège (Sart Tilman), Belgium.

|| Jožef Stefan Institute.

[1] Abbreviations: CD, circular dichroism; GdmCl, guanidinium chloride; PCR, polymerase chain reaction; UV, ultraviolet; ANS, 1-anilino-8-naphthalenesulfonate.

10.1021/bi701927y CCC: $40.75
Published on Web 01/03/2008

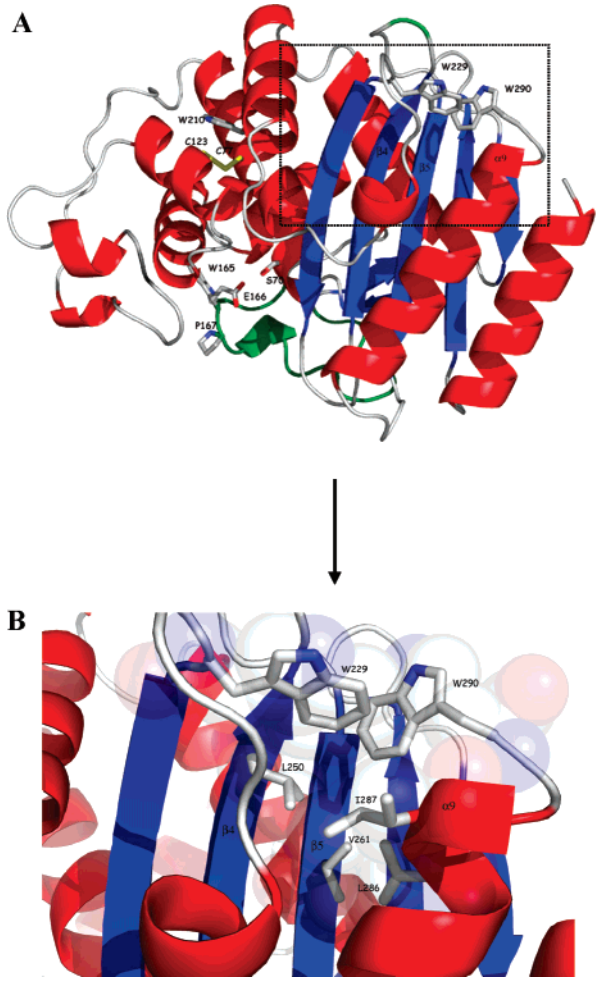

FIGURE 1: Schematic representation of the structure of the TEM-1 β-lactamase (*4*−*6*). (A) Ribbon representation with the secondary structure elements in the native structure highlighted in red (α-helices) and blue (β-strands). The Ω-loop and the disulfide bond are colored green and yellow, respectively. A few important residues and secondary structure elements (see the text) are indicated. (B) Enlarged view of the environment of Trp-220 and Trp-290 (i.e., the area in the box in panel A).

the burst phase. To gain further insight into these early kinetic folding events, we have constructed the W290F mutant of TEM-1 β-lactamase and characterized its folding properties in detail. Further evidence is presented supporting burial of the C-terminus of the polypeptide chain very early in the folding of the enzyme.

MATERIALS AND METHODS

Enzymes and Chemicals. Ultrapure guanidine chloride (GdmCl) was obtained from SERVA (Heidelberg, Germany). Benzylpenicillin was from Rhône-Polenc (Paris, France), cephalothin from Sigma Chemical Co., and cefotaxime from Roussel-Uclaf (Romainville, France). Other chemicals were reagent grade.

Wild-type TEM-1 β-lactamase was produced (*Escherichia coli* strain RB791) and purified as described by Dubus et al. (*12*). The W290F mutant was constructed using a two-step method including PCR and DpnI digestion (Quick Change site-directed mutagenesis kit, from Stratagene). For high-level expression, the corresponding gene was cloned into the pTac11Tc expression vector, using the BsaI and AlwNI restriction enzyme sites. The pTac11Tc vector is the pTac11 vector of Amann et al. (*13*) containing the tetracycline resistance gene. Recombinants containing the gene encoding W290F TEM-1 β-lactamase were thus detected on the basis of their ability to confer tetracycline resistance to *E. coli*. That no unwanted mutation was present in the W290F expression plasmid was confirmed by sequencing. Finally, *E. coli* strain JM109 was transformed by the pTac11Tc/W290F vector for overproduction and purification of the mutant enzyme, as described previously (*12*). This yielded ∼5−10 times less mutant enzyme than wild-type TEM-1.

Determination of Enzyme Kinetic Parameters. Kinetic parameters were determined at 30 °C in 50 mM sodium phosphate (pH 7) as for the wild-type enzyme (*14*), using a UVIKON 860 spectrophotometer (Kontron Instrument, Zürich, Switzerland).

Denaturant-Induced Unfolding Transitions. Equilibrium unfolding was studied at 25 °C in 50 mM sodium phosphate buffer, in the presence of 50 mM NaCl (pH 7). Samples at various GdmCl concentrations were left to equilibrate for at least 12 h [$t_{1/2}$ for TEM-1 unfolding in the presence of 0.9 M GdmCl of <10 min (*8*)]. Unfolding curves were determined by monitoring changes in intrinsic fluorescence emission (λ_{ex} = 280 nm; λ_{em} = 340 nm) and in far-UV CD at 220 nm, as described previously (*15*), using a Perkin-Elmer LS50B spectrofluorimeter and a Jobin-Yvon CD6 spectropolarimeter. Denaturant concentrations were determined from refractive index measurements (*16*), using a R5000 hand refractometer from Atago. Intrinsic fluorescence was measured at a protein concentration of ca. 0.015 mg mL^{-1} (0.4−0.5 μM), and concentrations of ca. 0.1 mg mL^{-1} (3 μM) were used in far-UV CD measurements.

Kinetics of Unfolding and Refolding in Manual Mixing Mode. All experiments were carried out at 25 °C in 50 mM sodium phosphate and 50 mM NaCl (pH 7). Kinetics of unfolding and refolding were measured by fluorescence spectroscopy as described for the wild-type enzyme (*8*), with a protein concentration of 0.4 μM. Refolding kinetics were also followed by estimating the recovery of enzymatic activity, as described for the wild-type enzyme (*8*), at a concentration of 0.2 μM. Double-jump experiments were performed as described previously (*8*). The dead time was ∼5−10 s.

Fluorescence Stopped-Flow Kinetics. A Bio-Logic (Claix, France) SFM-3 stopped-flow spectrometer was used, equipped with a 1.5 mm path length cell. The dead time was estimated to be in the range of 3−4 ms. Refolding reactions were initiated by an 11-fold dilution of the protein denatured in 3 M GdmCl [note that a 5 s incubation in 3 M GdmCl is sufficient to completely unfold the protein (*10*)], with refolding buffer. Changes in the intrinsic tryptophan fluorescence were followed by monitoring the total fluorescence above 320 nm (using a high-pass filter), with excitation at 280 nm (8 nm bandwidth). The final protein concentration was 3 μM. In all experiments, the photomultiplier voltage was set to 750 V, and 1000 data points were acquired over the time course of one experiment. Usually, five kinetic traces were averaged for one time constant ($\tau = 1/k$) measurement. The fluorescence yield of the unfolded protein (in 3 M GdmCl) was measured after an 11-fold dilution in a solution containing an equal concentration of denaturant. Thereafter, the fluorescence yield of the unfolded protein under refolding conditions (i.e., 0.273 M GdmCl) was estimated by extrapo-

lation, on the basis of that of the protein measured under equilibrium conditions at concentrations between 3 and 6 M.

Data Analysis. Equilibrium unfolding curves obtained by monitoring the intrinsic fluorescence of the protein were analyzed on the assumption of a two-state model (N ⇌ H) for the unfolding transition, according to eq 1. Corresponding data obtained by CD measurements were analyzed on the basis of a three-state model (N ⇌ H ⇌ U), using eq 2. Equations 1 and 2 are obtained by assuming that the differences in free energy between both the N and H species and the H and U species exhibit a linear dependence on denaturant concentration (*17*, *18*):

$$y_{obs} = [y_N + y_H \exp(a)]/[1 + \exp(a)] \quad (1)$$

$$y_{obs} = [y_N + \exp(a)\, y_H + \exp(a)\exp(b)\, y_U]/[1 + \exp(a) + \exp(a)\exp(b)] \quad (2)$$

where $a = -[\Delta G°(H_2O)_{N-H} + m_{N-H}[GdmCl]]/(RT)$ and $b = -[\Delta G°(H_2O)_{H-U} + m_{H-U}[GdmCl]]/(RT)$. y_{obs} is the measured parameter at a given denaturant concentration, and y_N, y_H, and y_U are the values of this parameter for the native, partially unfolded, and unfolded states, respectively, at the same denaturant concentration. The observed linear dependence of some of these parameters on denaturant concentration was taken into account, as described previously (*8*). $\Delta G°(H_2O)_{N-H}$ and $\Delta G°(H_2O)_{H-U}$ are the differences in free energy between N and H and between H and U, respectively, under physiological conditions; m_{N-H} and m_{H-U} are the slopes, $\delta(\Delta G°)/\delta[GdmCl]$, of the corresponding linear plots of the free energy against denaturant concentration. R is the gas constant and T the absolute temperature. The midpoints of the transitions, i.e., the denaturant concentrations at which [H]/[N] = 1 and [U]/[H] = 1, are given by the relationship $C_m = -\Delta G°(H_2O)/m$. The equilibrium folding data are presented as the fraction of the native protein signal (f_N) as a function of GdmCl concentration, calculated as follows (eq 3):

$$f_N = (y_U - y_{obs})/(y_U - y_N) \quad (3)$$

The kinetics of unfolding were analyzed according to a single-exponential term (eq 4). The kinetics of refolding were analyzed according to the sum of two (eq 5; slow kinetic experiments) or four (eq 6; fast kinetic experiments) exponential terms.

$$F_t = F_\infty + A \exp(-kt) \quad (4)$$

$$F_t = F_\infty + A_1 \exp(-k_1 t) + A_2 \exp(-k_2 t) \quad (5)$$

$$F_t = F_\infty + A_1 \exp(-k_1 t) + A_2 \exp(-k_2 t) + A_3 \exp(-k_3 t) + A_4 \exp(-k_4 t) \quad (6)$$

Grafit 3.09 (Erithacus Software Ltd.) was used for nonlinear least-squares analysis of the data. Errors are calculated as standard deviations throughout.

RESULTS

Enzymatic Activity Measurements. Values of the kinetic parameters for the mutant β-lactamase were measured with three substrates and do not differ significantly from those of the wild-type enzyme (Table 1).

Table 1: Kinetic Parameters for the W290F Mutant Enzyme at pH 7 and 30 °C[a]

substrate	k_{cat} (s^{-1})	K_m (μM)	k_{cat}/K_m ($mM^{-1}\ s^{-1}$)	k_{cat}/K_m (% of wild-type value)
benzylpenicillin	1400 (1600)	26 (19)	53000 (84000)	63
cephalotin	125 (160)	260 (250)	470 (650)	72
cefotaxime	nd[b] (9)	nd[b] (6000)	1.25 (1.5)	83

[a] Values in parentheses are for the wild-type enzyme (*14*). Standard deviations are on the order of 10−20% of the experimental values (n = 3). [b] Not detected.

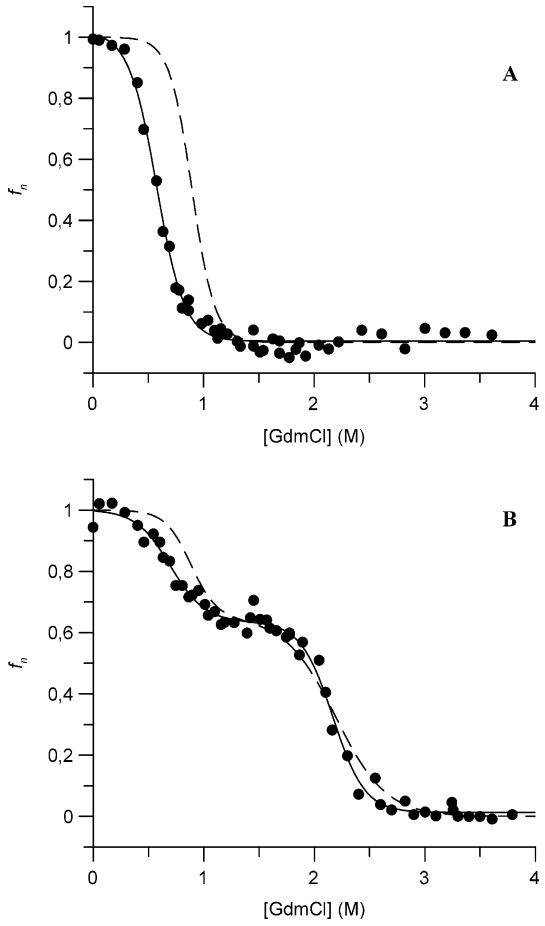

FIGURE 2: GdmCl-induced equilibrium unfolding transition of the W290F mutant at pH 7 and 25 °C monitored by (A) the change in fluorescence intensity at 340 nm and (B) the change in ellipticity at 220 nm. The data were analyzed on the basis of a three-state model, and the solid lines represent the best fits to eqs 1 (A) and 2 (B), calculated using the values of the thermodynamic parameters listed in Table 2. The dashed lines are the transitions obtained for the wild-type enzyme (*8*). Data are presented as the fraction of native signal (f_N, calculated according to eq 3), as a function of GdmCl concentration.

Chemical-Induced Unfolding. The stability of the W290F mutant was derived from GdmCl-induced denaturation of the protein (Figure 2). With both the wild-type and mutant enzymes, unfolding was found to be fully reversible and the noncoincidence of the transitions obtained by intrinsic fluorescence emission and far-UV CD measurements indicates that a stable intermediate species (H) is populated under equilibrium conditions. State H, which is thermodynamically stable in the presence of 1.5 M GdmCl for both the wild-

Table 2: Thermodynamic Parameters Characterizing Equilibrium Unfolding of Wild-Type and W290F TEM-1 β-Lactamases at pH 7 and 25 °C[a]

protein	$\Delta G°(H_2O)_{N-H}$[b] (kJ mol^{-1})	m_{N-H}[b] (kJ mol^{-1} M^{-1})	$C_{m,N-H}$[b] (M)	$\Delta G°(H_2O)_{H-U}$[c] (kJ mol^{-1})	m_{H-U}[c] (kJ mol^{-1} M^{-1})	$C_{m,H-U}$[c] (M)
W290F	12 ± 1	-20 ± 2	0.60 ± 0.03	30 ± 4	-17 ± 1	2.16 ± 0.03
wild type[d]	22 ± 2	-24 ± 2	0.90 ± 0.02	24 ± 1	-11 ± 0.4	2.24 ± 0.02

[a] The parameter values were calculated from panels A and B of Figure 2, using eqs 1 and 2. [b] From equilibrium unfolding followed by fluorescence spectroscopy. [c] From equilibrium unfolding followed by circular dichroism. [d] Values for the wild-type enzyme are from ref *8*.

type and mutant enzymes, has been described as a molten globule-like species (*8*).

Values of the thermodynamic parameters for the transitions (Table 2) were computed using eqs 1 and 2, assuming a three-state model. Substitution of Trp-290 with Phe resulted in a nonsignificant decrease in the free energy of N relative to U [$\Delta\Delta G°_{NU}$(WT-W290F) = 4 ± 5 kJ mol^{-1}]. Interestingly, however, the mutation destabilizes the native state by 10 ± 2 kJ mol^{-1} relative to the H state, and the latter is stabilized by 6 ± 4 kJ mol^{-1} relative to the unfolded state. The global *m* values of the mutant and wild-type enzymes are identical within the error limit ($m_{NU} \approx -36$ kJ mol^{-1} M^{-1}).

Unfolding and Refolding Kinetics: Slow Phases. Unfolding and refolding of the W290F mutant were monitored by fluorescence spectroscopy. With both proteins, unfolding kinetics were fitted by a single-exponential function (eq 4). At all concentrations that were tested, unfolding of the mutant protein is ~10 times faster than that of the wild-type species. In the presence of low denaturant concentrations, the refolding reactions were biphasic and experimental data could be fitted according to eq 5. The kinetics for the wild type and the W290F mutant, followed by the recovery of native fluorescence at 340 nm after manual mixing, are shown in Figure 3A. A typical biphasic renaturation curve is observed with both enzymes, and the values of the rate constants for the two phases [identified as phases 4 and 5 (*10*)] are identical within the error limit (Table 3). In the presence of GdmCl concentrations above 0.2 M for the mutant and 0.5 M for the wild type, however, the refolding reactions were monoexponential, and the kinetic traces were interpreted with eq 4. The refolding branch of the chevron plot (Figure 4) indicates that the folding rate constant values for the two proteins are similar and exhibit a similar marked dependence on GdmCl concentration.

The refolding of the W290F mutant protein followed at low GdmCl concentrations by measuring the recovery of enzyme activity (Figure 3B) is also biphasic, and the experimental data are in good agreement with the theoretical curve (i.e., a sum of two exponential functions, where $\tau_4 \approx 20$ s and $\tau_5 \approx 200$ s) obtained by Vanhove et al. (*8*) for the wild-type enzyme.

Finally, the two major slow phases observed with the TEM-1 β-lactamase have been shown, by double-jump experiments, to be associated with *cis*−*trans* isomerization of Xaa−Pro peptide bonds (*8*, *9*). Under the same experimental conditions, the two slow phases of the W290F mutant were also shown to be sensitive to double-mixing experiments (data not shown), hence indicating that both enzymes refold via two major parallel pathways (*9*), rate-limited by isomerization of the same proline residues.

Refolding Kinetics: Fast Phases. The refolding time courses of the wild-type and mutant enzymes (first 50 s), monitored by intrinsic fluorescence emission following stopped-flow mixing, are shown in panels A and B of Figure 5. The overall refolding of the TEM-1 β-lactamase monitored by intrinsic fluorescence exhibits six distinct phases, including the burst phase (phase 0) that takes place within the mixing dead time (3−4 ms) (*10*). We observed, similarly, the first four measurable phases (k_1−k_4) in the rapid mixing experiments (Figure 5A) and the last two phases (k_4 and k_5) in the manual mixing experiments (Figure 3). With the W290F mutant enzyme, the same number of measurable phases was observed, although phase 4 disappears at a GdmCl concentration higher than 0.2 M and is thus not seen in Figure 5B. The data in Figure 5 were fitted using the values of k_4 and k_5 obtained from the slow refolding experiments for the wild-type and mutant proteins, respectively. The accuracy of the fits can be assessed from the random distribution of residuals shown in Figure 5. When data were analyzed with only three exponentials, the accuracy of the fit was significantly poorer, as indicated by the distribution of residuals. Values of the refolding rate constants and corresponding amplitudes are listed in Table 4. The most noticeable feature is that the significant dead time burst observed with the wild-type β-lactamase, the amplitude of which accounts for ca. 20% of the total fluorescence change, is not observed with the W290F mutant enzyme.

After the dead time of the experiment, the two enzymes exhibited similar time courses for the change in exposure of tryptophans to solvent (Figure 5 and Table 4). Thus, in both cases, a significant decrease in fluorescence intensity, whose negative amplitude corresponded to 20−25% of the total fluorescence change, occurred in two phases to reach a minimum in ca. 800 ms, indicating a transient population of intermediate species with lower fluorescence quantum yield. Characterization of the C77A and C123A double mutant TEM-1 β-lactamase allowed Gervasoni and Plückthun (*7*) to assign this fluorescence quenching to the transfer of Trp-210 to its native topology, in a hydrophobic environment next to the enzyme disulfide bond (see Figure 1). This phase was followed by a relatively slow return of the fluorescence intensity to the value characteristic of the native state in two or three phases, depending on the experimental conditions. The different amplitudes for the corresponding phases (1−5), observed with the wild-type and mutant β-lactamases, are most probably due to the destabilization of the W290F mutant and to its different fluorescence properties, rather than to a qualitative change in the folding process.

DISCUSSION

To test the contribution of Trp-290 to the refolding kinetics of the TEM-1 β-lactamase, we initially constructed the W290L and W290R mutants. These, however, could not be

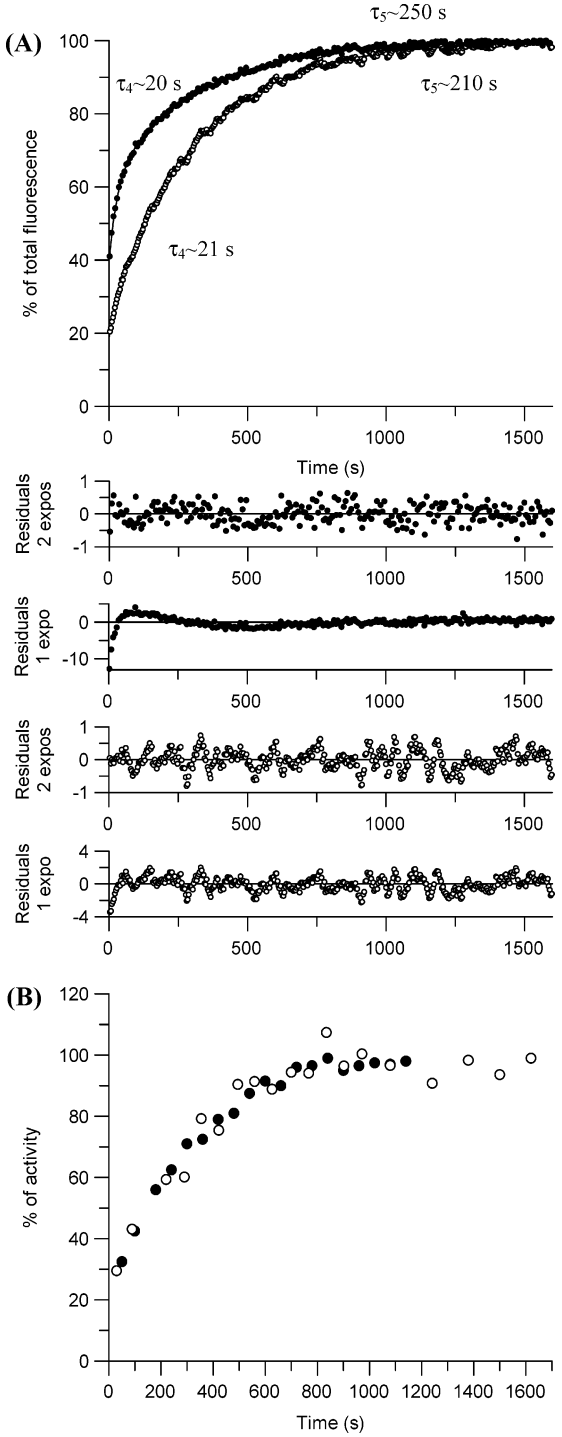

FIGURE 3: (A) Refolding kinetics of the wild type (●) and W290F mutant (○) of the TEM-1 β-lactamase at pH 7 and 25 °C in the presence of 0.15 M GdmCl, followed (A) by intrinsic fluorescence measurements and (B) by recovery of enzymatic activity. Fluorescence data have been fitted to double-exponential functions and normalized to the total fluorescence difference between the native and unfolded protein. The average time constant values were calculated from kinetic data in Table 3. In both cases, the pattern of residuals from the fit of the experimental data to single-exponential (1 expo) and double-exponential (2 expos) functions is shown for comparison. Enzymatic activity data for the wild-type enzyme are from ref *8*.

produced in *E. coli*, leading us to construct the W290F mutant. Production and purification of this mutant yielded reduced (5−10 times) quantities of protein in comparison with those obtained with the wild-type β-lactamase. These

Table 3: Kinetic Parameters for Fluorescence-Detected Refolding of TEM-1 β-Lactamase and the W290F Mutant after Manual Mixing in 0.15 M GdmCl at pH 7 and 25 °C[a]

protein	$A_{\text{dead time}}$ (%)	A_4 (%)	k_4 (s^{-1})	A_5 (%)	k_5 (s^{-1})
W290F	19 ± 3	5 ± 1	0.047 ± 0.004	76 ± 3	0.0047 ± 0.0005
wild type	40 ± 3	19 ± 2	0.050 ± 0.004	38 ± 2	0.0040 ± 0.0005

[a] The amplitude values (A) are normalized with respect to the total fluorescence change between the native and unfolded protein. All values are the averages of results from three consecutive refolding experiments.

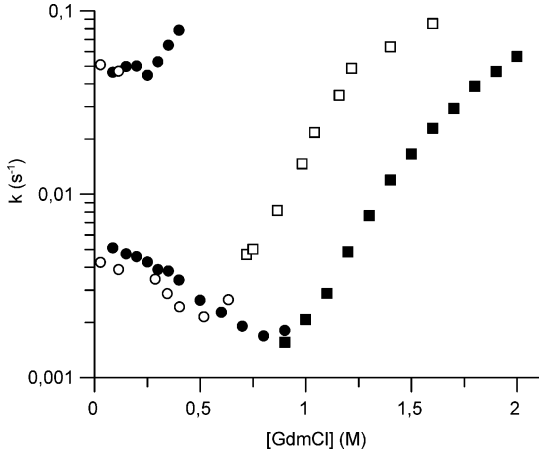

FIGURE 4: Apparent first-order rate constant values for unfolding (squares) and refolding (circles) of wild-type and W290F mutant β-lactamases: (empty symbols) W290F and (filled symbols) wild-type TEM-1. Rate constants were obtained by following changes in fluorescence intensity at 25 °C, in 50 mM sodium phosphate (pH 7) in the presence of 50 mM NaCl. Values for the wild-type protein are from ref *8*.

results suggest that an aromatic residue at position 290 is critical for correct in vivo folding of the enzyme but that the Trp to Phe substitution results in smaller production yields, probably for stability reasons (see below). In the native wild-type protein, the side chains of tryptophans 229 and 290 interact closely (a minimal distance of 3.8 Å is found between CH of Trp-229 and CE of Trp-290), with their indole rings roughly perpendicular to each other (Figure 1). Examination of nine three-dimensional structures of β-lactamases [TEM-1, PDB entry 1XPB (*6*); SHV-1, PDB entry 1SHV (*19*); *Mycobacterium fortuitum*, PDB entry 2CC1 (*20*); *Bacillus licheniformis* BS3, PDB entry 1I2S (*21*); PC1, PDB entry 1DJA (*22*); TOHO-1, PDB entry 1BZA (*23*); NMCA, PDB entry 1BUL (*24*); *Streptomyces albus G*, PDB entry 1BSG (*25*); and PER-1, PDB entry 1E25 (*26*)] indicates that a tryptophan residue is present at position 229 in seven of the enzymes (Tyr is present in *Streptomyces aureus* PC1 and Thr in *Pseudomonas aeruginosa* PER-1) and also reveals that residue 229 is always at van der Waals contact distance from a hydrophobic residue, either Trp-290 (in TEM-1 and SHV-1) or 287 (Leu in *B. licheniformis* BS3, Ile in NMCA, or Ala in *S. albus G*) or Leu-289 (in *M. fortuitum*). Furthermore, this interaction is part of a large hydrophobic cluster (Figure 1B) involving residues situated at the C-terminal end of the last α9 helix (e.g., Leu-286 and Ile-287 in TEM-1) and at the C- and N-terminal ends of strands β4 (Leu-250 in TEM-1) and β5 (Val-261 in TEM-1), respectively. These interactions are likely to stabilize the tertiary structure of the enzyme. Substitution of Trp-290 with Phe

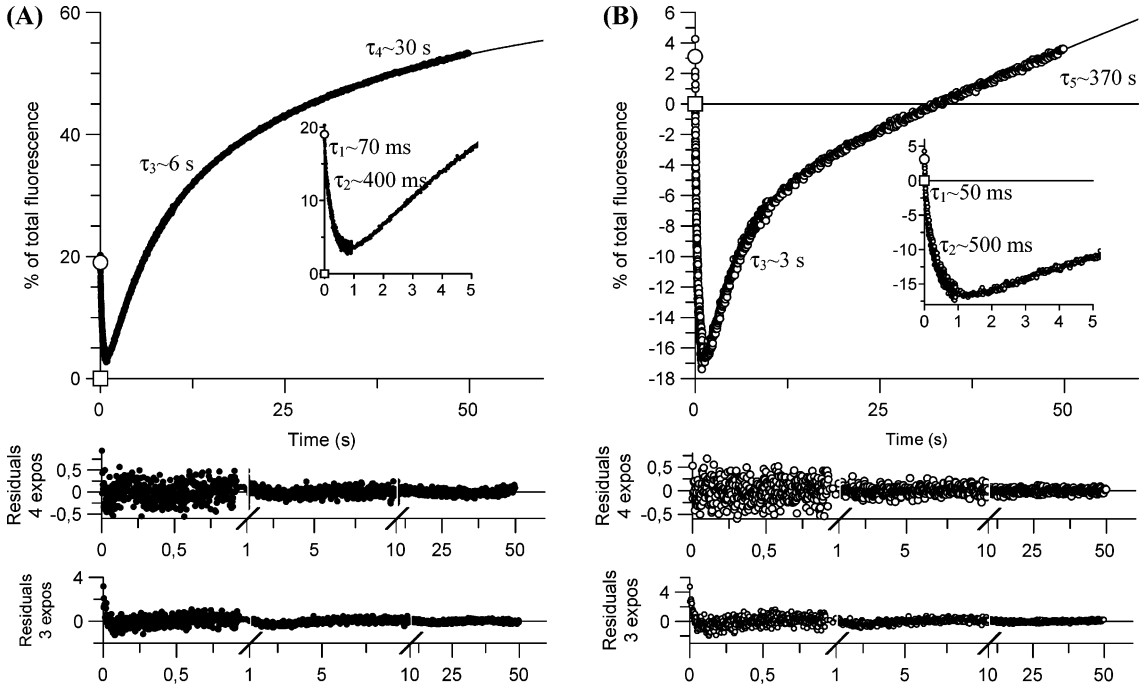

FIGURE 5: Refolding kinetics of wild-type TEM-1 (A) and W290F mutant (B) β-lactamases at pH 7 and 25 °C in the presence of 0.273 M GdmCl, monitored by intrinsic fluorescence after rapid mixing. $\lambda_{exc} = 280$ nm; $\lambda_{em} > 320$ nm. The fluorescence emission is normalized so that the value of the unfolded state under refolding conditions (see Materials and Methods) is 0 (indicated by □) and that of the native state is 100. The insets show the first 5 s of the reaction. Data have been fitted to the sum of four exponential functions (note that with the W290F mutant, phase 4 is not observed; see the text), and residuals from the fit of the experimental data to a sum of three-exponential (3 expos) and four-exponential (4 expos) functions are shown for comparison. The average time constant values were calculated from kinetic data listed in Table 4. (○) Intrinsic fluorescence intensity extrapolated to zero time from the kinetic data.

Table 4: Kinetic Parameters for Fluorescence-Detected Refolding of the TEM-1 β-Lactamase and the W290F Mutant after Fast Mixing (phases 0−3) and Manual Mixing (phases 4 and 5) in 0.273 M GdmCl at pH 7 and 25 °C[a]

protein	burst phase	phase 1	phase 2	phase 3	phase 4	phase 5
W290F *A* (%)	3 ± 2	−6 ± 1	−20 ± 3	15 ± 3	nd[b]	115 ± 7
k (s^{-1})	>500	19 ± 3	2.1 ± 0.1	0.21 ± 0.02	nd[b]	0.0027 ± 0.0002
wild-type *A* (%)	19 ± 3	−4 ± 1	−17 ± 2	24 ± 2	28 ± 2	43 ± 4
k (s^{-1})	>500	14 ± 2	2.5 ± 0.1	0.17 ± 0.01	0.033 ± 0.003	0.0031 ± 0.0003

[a] The amplitude values are normalized to the total fluorescence change between the native and unfolded protein. Values are averages of results from three consecutive refolding experiments, and in the fast mixing refolding mode, each result is the average of five refolding traces. [b] Not detected.

has no significant effect, however, on the specificity and catalytic activity of the β-lactamase, indicating that the mutation, which is far from the active site, has no influence on its structure. The optical properties of the enzyme (data not shown) further confirmed the lack of influence of the W290F mutation on the overall structure. The far-UV CD spectra of the wild-type and mutant proteins are indistinguishable, revealing that the indole group of Trp-290, despite its proximity to Trp-229, makes no significant contribution in the amide region (190−250 nm). This is different from the case of dihydrofolate reductase (*27*) and a number of other proteins (*28*), in which pairs of tryptophan side chains close to each other give rise to important CD bands in this region of the spectrum, due to electronic coupling ("exciton splicing") between the aromatic chromophores. In contrast with the far-UV CD data, intensities are reduced in the W290F mutant in the near-UV CD and intrinsic fluorescence spectra, but the overall shapes are the same, indicating that a stable and similar tertiary structure is maintained in the mutant enzyme. Notably, the maximum in fluorescence emission ($\lambda_{max} = 347$ nm) of the mutant is the same as that of the wild-type β-lactamase. The intrinsic fluorescence of TEM-1 is largely dominated by three of its four tryptophan residues (*10*) (see Figure 1), situated at positions 165, 229, and 290 [Trp-210 being largely quenched in the native state (*7*)]. This observation that removal of Trp-290 simply decreases the fluorescence intensity (by ∼20%) without shifting the maximum of the emission spectrum strongly suggests not only that the fluorescence contribution of Trp-290 similar to those of Trp-165 and 229 but also that the solvent accessibility of Trp-165 and Trp-229 is unchanged in the mutant protein. This observation, together with the strong negative signal observed in the near-UV region of the CD spectrum (not shown), indicates that the tertiary structure of the W290F mutant β-lactamase remains very similar to that of the wild-type enzyme. Taken together, all these observations demonstrate that the structure of the W290F TEM-1 β-lactamase is similar to that of the wild-type enzyme, even in the immediate neighborhood of the mutation.

W290F TEM-1 β-lactamase unfolds in a three-state transition, where a thermodynamically stable intermediate state H is significantly populated, as observed with the wild-type protein. The mutation, however, leads to a major

decrease (10 ± 2 kJ mol^{-1}) in the free energy difference between N and H, suggesting that the aromatic interaction between residues 229 and 290 is not firmly established in the dynamic tertiary structure characteristic of state H and thus that the mutation destabilizes the native state to a larger extent than the H state. This is consistent with the view that aromatic residues that are far apart in the sequence stabilize tertiary structure interactions (*29*).

Values of the first-order rate constants for the slow and very slow phases of refolding reactions of the wild-type and W290F TEM-1 β-lactamases, measured by fluorescence spectroscopy (Figure 4 and Table 3), indicate that the two major parallel pathways proposed by Vanhove et al. (*9*), both being rate-limited by isomerization of proline-containing peptide bonds (i.e., Xaa−Pro), are unaffected by the mutation.

Analysis of these data according to the protein engineering method developed by Fersht and co-workers (*30*, *31*) leads to $\Phi = 0$, suggesting that the polypeptide chain at the site of the mutation (i.e., position 290) exhibits a non-native fold in the transition state associated with the rate-limiting step along both folding routes. This is consistent with tryptophans 229 and 290 being brought into contact during the very late steps of the folding process of the wild-type enzyme (*10*). On the other hand, the ~10-fold increase in the unfolding rate constant values observed for the mutant protein (Figure 4) indicates that the native protein is destabilized by ca. 6 kJ mol^{-1} relative to the molten globule intermediate [$\Delta\Delta G^{\circ}_{N-H}$(WT-W290F) $= -RT \ln(k_{N-H}{}^{WT}/k_{N-H}{}^{W290F})$]. This is consistent with the values of the thermodynamic parameters in Table 2 and suggests that Phe-290 interacts substantially less strongly with Trp-229 than Trp-290 in the wild-type protein.

The rate constant and amplitude values of the first three measurable phases for the refolding process of the wild-type and mutant β-lactamases measured by fluorescence spectroscopy (Figure 5 and Table 4) are identical within the error limits, indicating that the mutation has no significant effect on these fast kinetic events. Most interestingly, however, the dead time increase in fluorescence intensity observed for the wild-type TEM-1 β-lactamase (Figure 5A) is no longer apparent with the W290F mutant (Figure 5B). With the wild-type enzyme (*10*), complementary fluorescence methods were used to monitor refolding. These experiments indicated that the burst phase intermediate is also characterized by significantly decreased access of acrylamide to aromatic residues and substantial ANS binding. The maximal binding of ANS actually occurs within the burst phase, a finding consistent with early hydrophobic collapse of the protein molecule. Changes in the quenching of fluorescence by acrylamide show that at least one of the four tryptophan residues encounters a significant change in its environment, resulting in a large increase in intrinsic fluorescence intensity, with lower accessibility to the solvent than in the native protein, in which they are largely exposed. The collapsed intermediate species formed at the onset of the refolding reaction thus contains non-native hydrophobic interactions involving tryptophan residues (*10*). Investigation of the folding kinetics of the W290F mutant suggests that the burst in the intrinsic fluorescence intensity observed with the wild-type enzyme can be assigned to the reduced level of exposure to solvent of the C-terminal W290 upon burial in a nonpolar environment at the onset of the refolding process. In the case of the W290F mutant β-lactamase, the fact that these non-native interactions involving the C-terminal end of the protein are not seen in the burst phase detected by intrinsic fluorescence is merely a consequence of the removal of the tryptophan residue at position 290.

Examination of the structural features of TEM-1 β-lactamase (Figure 1) and the Φ value associated with the mutation ($\Phi = 0$) suggests that Trp-290, and thus the C-terminal end of the enzyme, will not be in a native environment before the very last steps of the refolding process. This supports the proposal (*10*) that a major contribution to the increase in the intrinsic fluorescence intensity observed during the three slower phases results from formation of the close interaction of tryptophans 229 and 290 in the native state.

The non-native hydrophobic interactions observed in the folding of the TEM-1 enzyme are similar in essence to those demonstrated in the folding of hen lysozyme (*32*−*34*), where their subsequent disruption accounts for the rate-limiting step in the folding reaction. Although this is not the case with class A β-lactamases, the refolding of which is limited by *cis*−*trans* isomerization around Xaa−Pro peptide bonds, the occurrence of non-native interactions involving Trp-290 demonstrates that the folding of the TEM-1 β-lactamase is a nonhierarchical process.

ACKNOWLEDGMENT

We thank Dr. Marc Vanhove (Dyax, Liège, Belgium) for many enlightening discussions and for inspiration. We are grateful to Dr. Sylvie Goussard (Institut Pasteur, Unité des Agents Antibactériens, Paris, France) for kindly providing the plasmids encoding the TEM-1 mutants.

REFERENCES

1. Waley, S. G. (1992) in *The chemistry of β-lactams* (Page, M. I., Ed.) pp 198−228, Blackie Academic and Professional, London.
2. Frère, J. M. (1995) β-Lactamases and bacterial resistance to antibiotics, *Mol. Microbiol. 16*, 385−395.
3. Matagne, A., Dubus, A., Galleni, M., and Frère, J. M. (1999) The β-lactamase cycle: A tale of selective pressure and bacterial ingenuity, *Nat. Prod. Rep. 16*, 1−19.
4. Strynadka, N. C., Adachi, H., Jensen, S. E., Johns, K., Sielecki, A., Betzel, C., Sutoh, K., and James, M. N. (1992) Molecular structure of the acyl-enzyme intermediate in β-lactam hydrolysis at 1.7 Å resolution, *Nature 359*, 700−705.
5. Jelsch, C., Lenfant, F., Masson, J. M., and Samama, J. P. (1993) Crystal structure of *Escherichia coli* TEM1 β-lactamase at 1.8 Å resolution, *Proteins: Struct., Funct., Genet. 16*, 364−383.
6. Fonzé, E., Charlier, P., To'Th, Y., Vermeire, M., Raquet, X., Dubus, A., and Frère, J. M. (1995) TEM-1 β-lactamase structure solved by molecular replacement and refined structure of the S235A mutant, *Acta Crystallogr. D51*, 682−694.
7. Gervasoni, P., and Plückthun, A. (1997) Folding intermediates of β-lactamase recognized by GroEL, *FEBS Lett. 401*, 138−142.
8. Vanhove, M., Raquet, X., and Frère, J. M. (1995) Investigation of the folding pathway of the TEM-1 β-lactamase, *Proteins: Struct., Funct., Genet. 22*, 110−118.
9. Vanhove, M., Raquet, X., Palzkill, T., Pain, R. H., and Frère, J. M. (1996) The rate-limiting step in the folding of the *cis*-Pro167Thr mutant of TEM-1 β-lactamase is the *trans* to *cis* isomerization of a non-proline peptide bond, *Proteins: Struct., Funct., Genet. 25*, 104−111.
10. Vanhove, M., Lejeune, A., Guillaume, G., Virden, R., Pain, R. H., Schmid, F. X., and Frère, J. M. (1998) A collapsed intermediate with non-native packing of hydrophobic residues in the folding of TEM-1 β-lactamase, *Biochemistry 37*, 1941−1950.

11. Dobson, C. M., Sali, A., and Karplus, M (1998) Protein Folding: A Perspective from Theory and Experiment, *Angew. Chem., Int. Ed. 37*, 868−893.
12. Dubus, A., Wilkin, J. M., Raquet, X., Normark, S., and Frère, J. M. (1994) Catalytic mechanism of active-site serine β-lactamases: Role of the conserved hydroxy group of the Lys-Thr-(Ser)-Gly triad, *Biochem. J. 301*, 485−494.
13. Amann, E., Brosius, J., and Ptashne, M. (1983) Vectors bearing a hybrid trp-lac promoter useful for regulated expression of cloned genes in *Escherichia coli*, *Gene 25*, 167−178.
14. Raquet, X., Lamotte-Brasseur, J., Fonzé, E., Goussard, S., Courvalin, P., and Frère, J. M. (1994) TEM β-lactamase mutants hydrolysing third-generation cephalosporins. A kinetic and molecular modelling analysis, *J. Mol. Biol. 244*, 625−639.
15. Dumoulin, M., Conrath, K., Van Meirhaeghe, A., Meersman, F., Heremans, K., Frenken, L. G., Muyldermans, S., Wyns, L., and Matagne, A. (2002) Single-domain antibody fragments with high conformational stability, *Protein Sci. 11*, 500−515.
16. Nozaki, Y. (1972) The preparation of guanidine hydrochloride, *Methods Enzymol. 26*, 43−51.
17. Santoro, M. M., and Bolen, D. W. (1988) Unfolding free energy changes determined by the linear extrapolation method. 1. Unfolding of phenylmethanesulfonyl α-chymotrypsin using different denaturants, *Biochemistry 27*, 8063−8068.
18. Pace, C. N. (1990) Measuring and increasing protein stability, *Trends Biotechnol. 8*, 93−98.
19. Kuzin, A. P., Nukaga, M., Nukaga, Y., Hujer, A. M., Bonomo, R. A., and Knox, J. R. (1999) Structure of the SHV-1 β-lactamase, *Biochemistry 38*, 5720−5727.
20. Sauvage, E., Fonzé, E., Quinting, B., Galleni, M., Frère, J. M., and Charlier, P. (2006) Crystal structure of the *Mycobacterium fortuitum* class A β-lactamase: Structural basis for broad substrate specificity, *Antimicrob. Agents Chemother. 50*, 2516−2521.
21. Fonzé, E., Vanhove, M., Dive, G., Sauvage, E., Frère, J. M., and Charlier, P. (2002) Crystal structures of the *Bacillus licheniformis* BS3 class A β-lactamase and of the acyl-enzyme adduct formed with cefoxitin, *Biochemistry 41*, 1877−1885.
22. Chen, C. C., Smith, T. J., Kapadia, G., Wäsch, S., Zawadzke, L. E., Coulson, A., and Herzberg, O. (1996) Structure and kinetics of the β-lactamase mutants S70A and K73H from *Staphylococcus aureus* PC1, *Biochemistry 35*, 12251−12258.
23. Ibuka, A., Taguchi, A., Ishiguro, M., Fushinobu, S., Ishii, Y., Kamitori, S., Okuyama, K., Yamaguchi, K., Konno, M., and Matsuzawa, H. (1999) Crystal structure of the E166A mutant of extended-spectrum β-lactamase Toho-1 at 1.8 Å resolution, *J. Mol. Biol. 285*, 2079−2087.
24. Mourey, L., Swaren, P., Miyashita, K., Bulychev, A., Mobashery, S., and Samama, J. P. (1998) Inhibition of the Nmc-A β-lactamase by a penicillanic acid derivative, and the structural bases for the increase in substrate profile of this antibiotic resistance enzyme, *J. Am. Chem. Soc. 120*, 9382−9383.
25. Dideberg, O., Charlier, P., Wery, J. P., Dehottay, P., Dusart, J., Erpicum, T., Frère, J. M., and Ghuysen, J. M. (1987) The crystal structure of the β-lactamase of *Streptomyces albus* G at 0.3 nm resolution, *Biochem. J. 245*, 911−913.
26. Tranier, S., Bouthors, A. T., Maveyraud, L., Guillet, V., Sougakoff, W., and Samama, J. P. (2000) The high resolution crystal structure for class A β-lactamase PER-1 reveals the bases for its increase in breadth of activity, *J. Biol. Chem. 275*, 28075−28082.
27. Kuwajima, K., Garvey, E. P., Finn, B. E., Matthews, C. R., and Sugai, S. (1991) Transient intermediates in the folding of dihydrofolate reductase as detected by far-ultraviolet circular dichroism spectroscopy, *Biochemistry 30*, 7693−7703.
28. Woody, R. W., and Dunker, A. K. (1996) Aromatic and cystein side-chain circular dichroism in proteins, in *Circular dichroism and the conformational analysis of biomolecules* (Fasman, G. D., Ed.) pp 159−182, Plenum, New York.
29. Thomas, A., Meurisse, R., Charloteaux, B., and Brasseur, R. (2002) Aromatic side-chain interactions in proteins. I. Main structural features, *Proteins: Struct., Funct., Genet. 48*, 628−634.
30. Matouschek, A., Kellis, J. T., Jr., Serrano, L., and Fersht, A. R. (1989) Mapping the transition state and pathway of protein folding by protein engineering, *Nature 340*, 122−126.
31. Fersht, A. R. (1999) Protein Stability, in *Structure and mechanism in protein science: A guide to enzyme catalysis and protein folding*, pp 558−563, W. H. Freeman and Co., New York.
32. Radford, S. E., Dobson, C. M., and Evans, P. A. (1992) The folding pathway of hen lysozyme involves partially structured intermediates and multiple pathways, *Nature 358*, 302−307.
33. Rothwarf, D. M., and Scheraga, H. A. (1996) Role of non-native aromatic and hydrophobic interactions in the folding of hen egg white lysozyme, *Biochemistry 35*, 13797−13807.
34. Matagne, A., Chung, E. W., Ball, L. J., Radford, S. E., Robinson, C. V., and Dobson, C. M. (1998) The origin of the α-domain intermediate in the folding of hen lysozyme, *J. Mol. Biol. 277*, 997−1005.

BI701927Y